

# Quantum Rabi model for two qubits

**S. A. Chilingaryan**

Departamento de Física, Universidade Federal de Minas Gerais, caixa postal 702,  
30123-970, Belo Horizonte, MG, Brazil

E-mail: suren@ufmg.br

**B. M. Rodríguez-Lara**

Instituto Nacional de Astrofísica, Óptica y Electrónica  
Calle Luis Enrique Erro No. 1, Sta. Ma. Tonantzintla, Pue. CP 72840, México

E-mail: bmlara@inaoep.mx

**Abstract.** We study the two-qubit Rabi model in the most general case where the qubits are different from each other. The spectrum of the system in the ultrastrong-coupling regime is shown to converge to two forced oscillator chains by perturbation theory. An even and odd decomposition of the Hilbert space allows us to calculate the spectra in any given parameter regime; the cases studied confirm our perturbation theory prediction in the ultrastrong-coupling regime and point to crossings in the spectra within each parity subspace in the moderate-coupling regime. The normal modes of the system are calculated by two different methods, the first a linear algebra approach via the parity bases that delivers a four-term recurrence relation for the amplitudes of the proper states and, the second, via Bargmann representation for the field that delivers five-term recurrence relations. Finally, we show some examples of the time evolution of the mean photon number, population inversion, von Neuman entropy and Wootters concurrence under the two-qubit quantum Rabi Hamiltonian by taking advantage of the parity decomposition.

PACS numbers: 03.65.Ge, 42.50.Ct, 42.50.Pq

## 1. Introduction

The Dicke model [1] is the simplest model describing the interaction of an ensemble of identical two-level systems with a boson field under the rotating wave approximation. In units of  $\hbar$ , it is written as:

$$\hat{H}_D = \omega_f \hat{a}^\dagger \hat{a} + \omega_0 \hat{J}_z + g \left( \hat{a} \hat{J}_+ + \hat{a}^\dagger \hat{J}_- \right), \quad (1)$$

where the field mode of frequency  $\omega_f$  is described by creation (annihilation) operators  $\hat{a}^\dagger$  ( $\hat{a}$ ) and the identical two-level systems or qubits with transition frequency  $\omega_0$  are described by collective Dicke or angular momentum operators answering the  $su(2)$  algebra,  $[\hat{J}_z, \hat{J}_\pm] = \pm \hat{J}_\pm$  and  $[\hat{J}_+, \hat{J}_-] = 2\hat{J}_z$ , the ensemble-field coupling is given by the parameter  $g$ . The Dicke model, also known as Tavis-Cummings model [2], is exactly solvable and has successfully used to describe super-radiance, super-fluorescence and amplified spontaneous emission phenomena in cavity-quantum electrodynamics (cavity-QED), ion-trap cavity-QED, and circuit-QED systems; see [3] for a review.

Without the rotating wave approximation (RWA) and in units of  $\hbar$ ,

$$\hat{H}_R = \omega_f \hat{a}^\dagger \hat{a} + \omega_0 \hat{J}_z + g \left( \hat{a} + \hat{a}^\dagger \right) \left( \hat{J}_+ + \hat{J}_- \right), \quad (2)$$

the Dicke model has recently been known as the quantum Rabi model. For many years the quantum Rabi model was a mathematical curiosity, as dipole-field systems cannot reach the strong-coupling regime in a simple way; e.g., the proposed and experimental realizations to find the quantum phase transition in the ground state of the Dicke model [4, 5, 6, 7]. Nevertheless, the proper system, dynamics and the notion of integrability of a single two-level system interacting with a single mode boson field without the RWA was studied utilizing Bargman representation [8], continued fractions [9, 10, 11], semi-classical methods [12], perturbation theory [13, 14], and coupled cluster [15] methods. It has also been discussed in the literature the influence of the so-called counter-rotating terms eliminated by the RWA on the phase distribution of a micromaser cavity field [16], on the quantum Zeno and anti-Zeno effects [17] and on the linear polarizability [18]. Recently, the interest on the single qubit Rabi model has been relighted due to the ability of solid-state-cavity-QED [19] and circuit-QED [20, 21] systems to attain the strong-coupling regime where the RWA fails. Thus, the single qubit Rabi model has been revisited using perturbation theory [22, 23], continued fractions [24, 25], Bargmann representation [26, 27, 28, 29, 30, 31], and coherent states [32] methods.

Here, we are interested in the quantum Rabi model for two nonidentical qubits, described by the Pauli operators  $\hat{\sigma}_j^{(k)}$  with  $j = x, y, z$  and  $k = 1, 2$  and the transition frequencies  $\omega_1$  and  $\omega_2$ ,

$$\hat{H} = \omega_f \hat{a}^\dagger \hat{a} + \frac{1}{2} \left( \omega_1 \hat{\sigma}_z^{(1)} + \omega_2 \hat{\sigma}_z^{(2)} \right) + \left( \hat{a} + \hat{a}^\dagger \right) \left( g_1 \hat{\sigma}_x^{(1)} + g_2 \hat{\sigma}_x^{(2)} \right), \quad (3)$$

which, up to our knowledge, has only been studied in a simplified form where the transition frequency of one of the qubit is set to zero [33]. The model (3) conserves parity defined as

$$\hat{\Pi} = \hat{\sigma}_z^{(1)} \hat{\sigma}_z^{(2)} (-1)^{\hat{a}^\dagger \hat{a}}, \quad (4)$$

i.e.,  $[\hat{\Pi}, \hat{H}] = 0$ , and may be of interest to the circuit-QED community where it has been used in the weak-coupling regime under the RWA for coherent quantum storage and transfer between two phase qubits [34] and for resonant two-qubit phase gates [35]; the validity of the latter breaks in the ultrastrong-coupling regime where the full quantum Rabi model has to be used [36]. The effect of counter rotating terms on entanglement and discord in a lossy two-qubit Rabi system has also been studied numerically [37].

In the following, we discuss the eigenvalues of Hamiltonian (3) in both the weak- and strong-coupling regimes. The eigenvalues are exact in the former and approximated up to second order correction by using perturbation theory in the latter. We take advantage of parity conservation to numerically calculate the spectra in each of the parity subspaces. Then, we present the proper functions via linear algebra methods and functions in Bargmann representation [38]. In the second to last section, we show how the time evolution in the weak-coupling regime can be calculated in closed form and how to calculate the evolution of quantities of interest in the parity decomposition. Finally, we close with a brief conclusion.

## 2. Eigenvalues of the model

In this section we calculate the exact eigenvalues for the system in the weak-coupling regime by partitioning the Hilbert space into subspaces described by the total excitation number. In the strong-coupling regime, we use perturbation theory to approximate the eigenvalues to second order correction.

### 2.1. Weak-coupling regime

It is quite trivial to calculate the eigenvalues of the general two-qubit quantum Rabi model (3) in the weak-coupling regime,  $g_1, g_2 \ll \omega_f$ , where the RWA approximation is valid,

$$\hat{H}_{RWA} = \omega_f \hat{a}^\dagger \hat{a} + \frac{1}{2} \sum_{j=1,2} \omega_j \hat{\sigma}_z^{(j)} + \sum_{j=1,2} g_j \left( \hat{a} \hat{\sigma}_+^{(j)} + \hat{a}^\dagger \hat{\sigma}_-^{(j)} \right), \quad (5)$$

In this regime, we can find the eigenvalues by partitioning the Hilbert space into subspaces with a well defined total excitation number,  $\hat{N} = \hat{n} + (\hat{\sigma}_z^{(1)} + \hat{\sigma}_z^{(2)})/2$ ; for example, for zero excitation the eigenstate is  $|0, g, g\rangle$  with energy  $\lambda_0 = -(\omega_1 + \omega_2)/2$ , for one excitation the subspace is spanned by  $\{|1, g, g\rangle, |0, g, e\rangle, |0, e, g\rangle\}$ , and for the rest,  $n \geq 2$ , the corresponding subspace is spanned by  $\{|n, g, g\rangle, |n-1, g, e\rangle, |n-1, e, g\rangle, |n-2, e, e\rangle\}$ .

Figure (1) shows the exact spectra in the RWA versus the numerical spectra for the whole Hamiltonian considering up to one thousand excitations in the system. We present in Fig. 1(a) the on-resonance case for equal qubits,  $\omega_1 = \omega_2 = \omega_f$ , and equal couplings  $g_1 = g_2 = g \in [0, 0.15]\omega_f$ . Figure 1(b) shows the case presented in [33], where one of the qubits has zero self-energy and the quantum field is detuned to the blue of the qubit with nonzero transition frequency,  $\omega_1 = 0.7\omega_f$  and  $\omega_2 = 0$ , and equal couplings,  $g_1 = g_2 = g \in [0, 0.15]\omega_f$ . The case for symmetric detuning,  $\omega_1 = 0.9\omega_f$  and  $\omega_2 = 1.1\omega_f$ ,

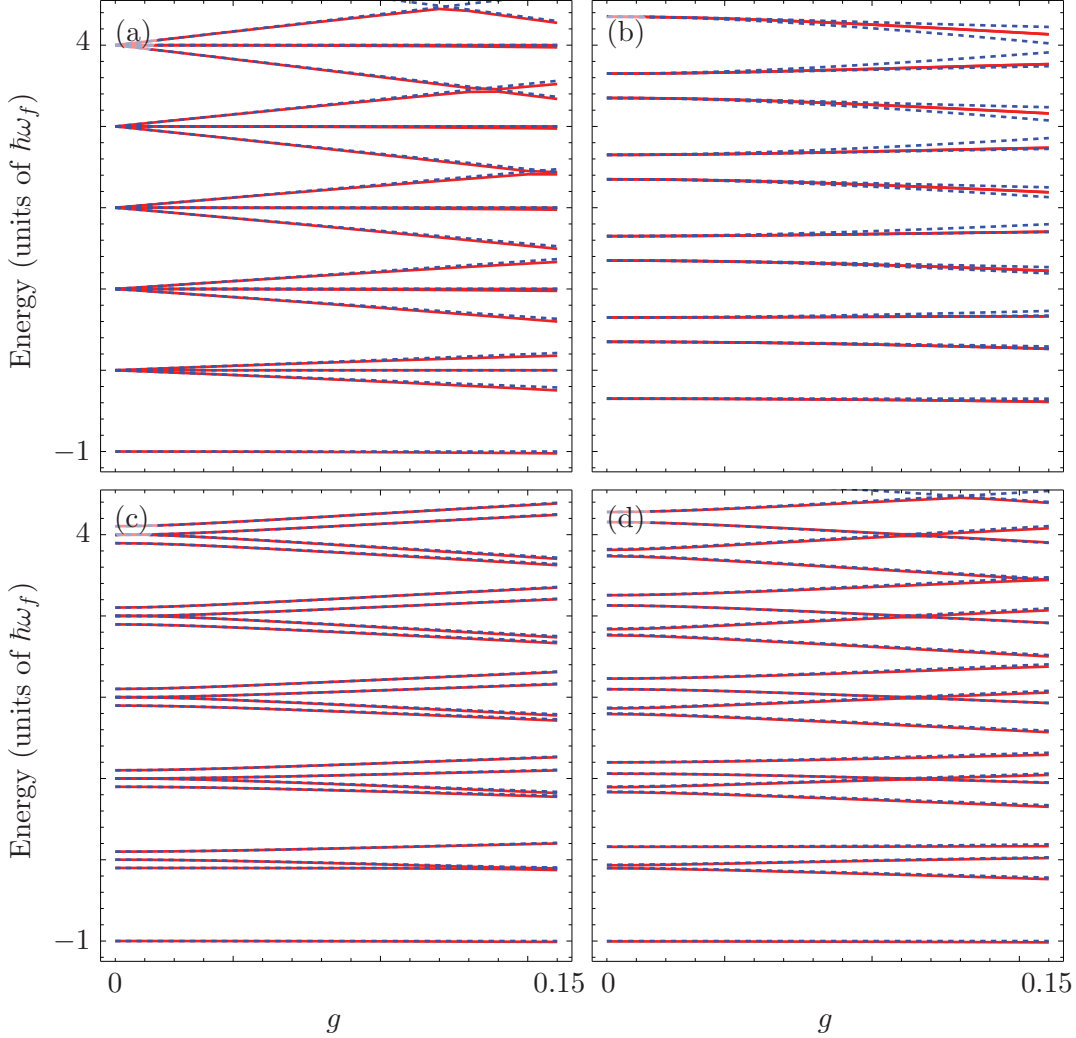


**Figure 1.** (Color online) Exact spectra in the rotating-wave approximation (dashed blue) and numerical spectra for the quantum Rabi Hamiltonian considering a subspace of up to one thousand excitations (solid red) for different parameter sets:  $\{\omega_1, \omega_2, g_1, g_2\} =$  (a)  $\{1, 1, g, g\}\omega_f$ , (b)  $\{0.7, 0, g, g\}\omega_f$ , (c)  $\{0.9, 1.1, 0.01, g\}\omega_f$ , and (d)  $\{1.1, 0.9, 0.1, g\}\omega_f$ .

with the first qubit coupled to the field at a fixed coupling value  $g_1 = 0.01\omega_f$  and variable coupling parameter for the other qubit,  $g_2 = g \in [0, 0.15]\omega_f$ , is shown in Fig.1(c). We show a similar case,  $\omega_1 = 1.1\omega_f$  and  $\omega_2 = 0.9\omega_f$ ,  $g_2 = g \in [0, 0.15]\omega_f$ , with a slightly larger fixed coupling,  $g_1 = 0.1\omega_f$  in Fig. 1(d). One can see that it is safe to say that the exact eigenvalues in the RWA describe well the spectra when the relation between the coupling strengths and the field frequency is below 10%,  $g_j/\omega_f < 0.1$ , [36] but some particular cases may extend further this range in one coupling by restricting the other; e.g., Figure 1(c) and 1(d). Notice that the RWA fails to describe the anti-crossings in the quantum Rabi spectra; e.g., Figure 1(a) and 1(d).

## 2.2. Strong-coupling regime

In order to approximate the eigenvalues in this regime, let us assume that the coupling parameters are larger than the transition frequencies,  $g_1, g_2 \gg \omega_1, \omega_2$ . In such a case, we can write the two-qubit quantum Rabi model (3) as a leading Hamiltonian with a perturbation,  $\hat{H} = \hat{H}_0 + \hat{P}$ , where

$$\hat{H}_0 = \omega_f \hat{n} + (\hat{a} + \hat{a}^\dagger) (g_1 \hat{\sigma}_x^{(1)} + g_2 \hat{\sigma}_x^{(2)}), \quad (6)$$

$$\hat{P} = \frac{1}{2} (\omega_1 \hat{\sigma}_z^{(1)} + \omega_2 \hat{\sigma}_z^{(2)}). \quad (7)$$

At this point we can use the transformation

$$\hat{R}_y = e^{-i\hat{\sigma}_y^{(1)}\theta} \otimes e^{-i\hat{\sigma}_y^{(2)}\theta} \quad (8)$$

with  $\theta = \pi/4$  to implement the changes  $\hat{\sigma}_x^{(j)} \rightarrow \hat{\sigma}_z^{(j)}$  and  $\hat{\sigma}_z^{(j)} \rightarrow -\hat{\sigma}_x^{(j)}$  leading to the form,

$$\tilde{H}_0 = \omega_f \hat{n} + (\hat{a} + \hat{a}^\dagger) (g_1 \hat{\sigma}_z^{(1)} + g_2 \hat{\sigma}_z^{(2)}), \quad (9)$$

$$\tilde{P} = -\frac{1}{2} (\omega_1 \hat{\sigma}_x^{(1)} + \omega_2 \hat{\sigma}_x^{(2)}), \quad (10)$$

where the tilde has been used to represent the rotated operator,  $\tilde{O} = \hat{R}_y^\dagger(\pi/4) \hat{O} \hat{R}_y(\pi/4)$ . Notice that the unperturbed Hamiltonian  $\tilde{H}_0$  can be diagonalized,

$$\tilde{H}_0 = \hat{T}_D \left[ \omega_f \hat{n} - \frac{1}{\omega_f} \begin{pmatrix} g_+^2 & 0 & 0 & 0 \\ 0 & g_-^2 & 0 & 0 \\ 0 & 0 & g_-^2 & 0 \\ 0 & 0 & 0 & g_+^2 \end{pmatrix} \right] \hat{T}_D^\dagger, \quad (11)$$

by using a driven oscillator basis provided by the transformation

$$\hat{T}_D = \begin{pmatrix} \hat{D}(g_+/\omega_f) & 0 & 0 & 0 \\ 0 & \hat{D}(g_-/\omega_f) & 0 & 0 \\ 0 & 0 & \hat{D}(-g_-/\omega_f) & 0 \\ 0 & 0 & 0 & \hat{D}(-g_+/\omega_f) \end{pmatrix}, \quad (12)$$

where the displacement operator is defined as  $\hat{D}(\alpha) = e^{\alpha \hat{a}^\dagger - \alpha^* \hat{a}}$  fulfilling  $\hat{D}^\dagger(\alpha) = \hat{D}(-\alpha)$  and  $\hat{D}(\alpha) \hat{D}(\beta) = \hat{D}(\alpha + \beta)$ . The auxiliary coupling parameters are defined as  $g_\pm = g_1 \pm g_2$ . Thus, we have the zeroth order approximated eigenvalues in the strong-coupling regime,

$$\epsilon_{1,m} = \epsilon_{4,m} \approx \omega_f m - \frac{g_+^2}{\omega_f}, \quad (13)$$

$$\epsilon_{2,m} = \epsilon_{3,m} \approx \omega_f m - \frac{g_-^2}{\omega_f}, \quad (14)$$

that happen to be two-fold degenerate. The first order correction due to the perturbation  $\tilde{P}$  is null due to the lack of diagonal components in the driven oscillator basis,

$$\hat{T}_D \tilde{P} \hat{T}_D^\dagger = \begin{pmatrix} 0 & \omega_2 \hat{D}(2g_2/\omega_f) & \omega_1 \hat{D}(2g_1/\omega_f) & 0 \\ \omega_2 \hat{D}(-2g_2/\omega_f) & 0 & 0 & \omega_1 \hat{D}(2g_1/\omega_f) \\ \omega_1 \hat{D}(-2g_1/\omega_f) & 0 & 0 & \omega_2 \hat{D}(2g_2/\omega_f) \\ 0 & \omega_1 \hat{D}(-2g_1/\omega_f) & \omega_2 \hat{D}(-2g_2/\omega_f) & 0 \end{pmatrix},$$

(15)

but the second order corrections are available leading to the approximate eigenvalues,

$$\epsilon_{1,m} = \epsilon_{4,m} \approx \omega_f m - \frac{g_+^2}{\omega_f} - \epsilon_{2,+}, \quad (16)$$

$$\epsilon_{2,m} = \epsilon_{3,m} \approx \omega_f m - \frac{g_-^2}{\omega_f} - \epsilon_{2,-}, \quad (17)$$

where the second order correction is given by

$$\epsilon_{2,\pm} = \sum_{m \neq n} \frac{\omega_1^2 |\langle m | \hat{D}(2g_1/\omega_f) | n \rangle|^2}{\omega_f(m-n) \pm 4g_1g_2/\omega_f} + \sum_{m \neq n} \frac{\omega_2^2 |\langle m | \hat{D}(2g_2/\omega_f) | n \rangle|^2}{\omega_f(m-n) \pm 4g_1g_2/\omega_f}. \quad (18)$$

Notice that for extremely large values of the coupling parameters  $g_1$  and  $g_2$ , i.e., ultrastrong-coupling, the second order corrections tend to zero and each of the spectral branches of the two-qubit quantum Rabi model, (16) and (17), tends to the spectra of a forced oscillator. For large values of the coupling parameters  $g_1, g_2 \gg \omega_1, \omega_2$ , we can calculate the second order correction by using the identity  $\langle m | \hat{D}(2x) | n \rangle = \sqrt{\frac{m!}{n!}} (2x)^{(m-n)} e^{-2|x|^2} \mathcal{L}_n^{(m-n)}(|2x|^2)$  where  $\mathcal{L}_a^{(b)}(z)$  is the  $b$ th generalized Laguerre polynomial.

Figure 2 shows the numerical spectra for the quantum Rabi Hamiltonian expanded in the parity subspaces span by the even, (21), and odd, (22), parity basis defined in the following section. We consider up to a thousand excitations in the system; i.e., truncated  $H_{\pm}$  matrices given by (23) of size one thousand with coupling steps of one hundredth of the field frequency,  $\Delta g = 0.01 \omega_f$ . In Fig.2(a) and (b), we show the symmetric off-resonance case,  $\omega_1 = 1.3 \omega_f$  and  $\omega_2 = 0.7 \omega_f$ , with identical couplings,  $g_1 = g_2 = g \in [0, 2]\omega_f$ . The spectra corresponding to even parity eigenvectors is presented as solid red lines and that corresponding to odd parity as dashed blue lines. The inset in Fig. 2(a) shows an energy crossing in the even spectra confirmed by comparison of the proper states before and after the crossing. The spectra in the moderate coupling region is presented in Fig. 2(b).

Figure 2(c) and (d) shows the numerical spectra for the quantum Rabi Hamiltonian for the case presented in [33]; i.e., blue detuned field with the transition frequency of one qubit being negligible,  $\omega_1 = 0.7\omega_f$  and  $\omega_2 = 0$ , and identical couplings,  $g_1 = g_2 = g \in [0, 2]\omega_f$ . Again, solid red lines correspond to the spectra of the even parity subspace and dashed blue lines to that in the odd parity subspace. We present a magnification of this case in the moderate coupling region in 2(d). Note that the even and odd spectra are completely degenerate. Energy crossings appeared at some parts of the spectra in all the cases studied; i.e., we looked at the first fifty eigenvalues by using a random transition frequency  $\omega_1 \in (0, 2]\omega_f$  and confirmed crossings by comparing the eigenvectors before and after the apparent crossing.

We also studied a variety of cases not shown here; e.g. random qubit transition energies  $\omega_1, \omega_2 \in [0, 2]\omega_f$  with identical couplings  $g_1 = g_2 = g$  or one fixed random coupling  $g_1 \in [0, 2]\omega_f$ . In all the cases studied, energy crossings in the spectra of each

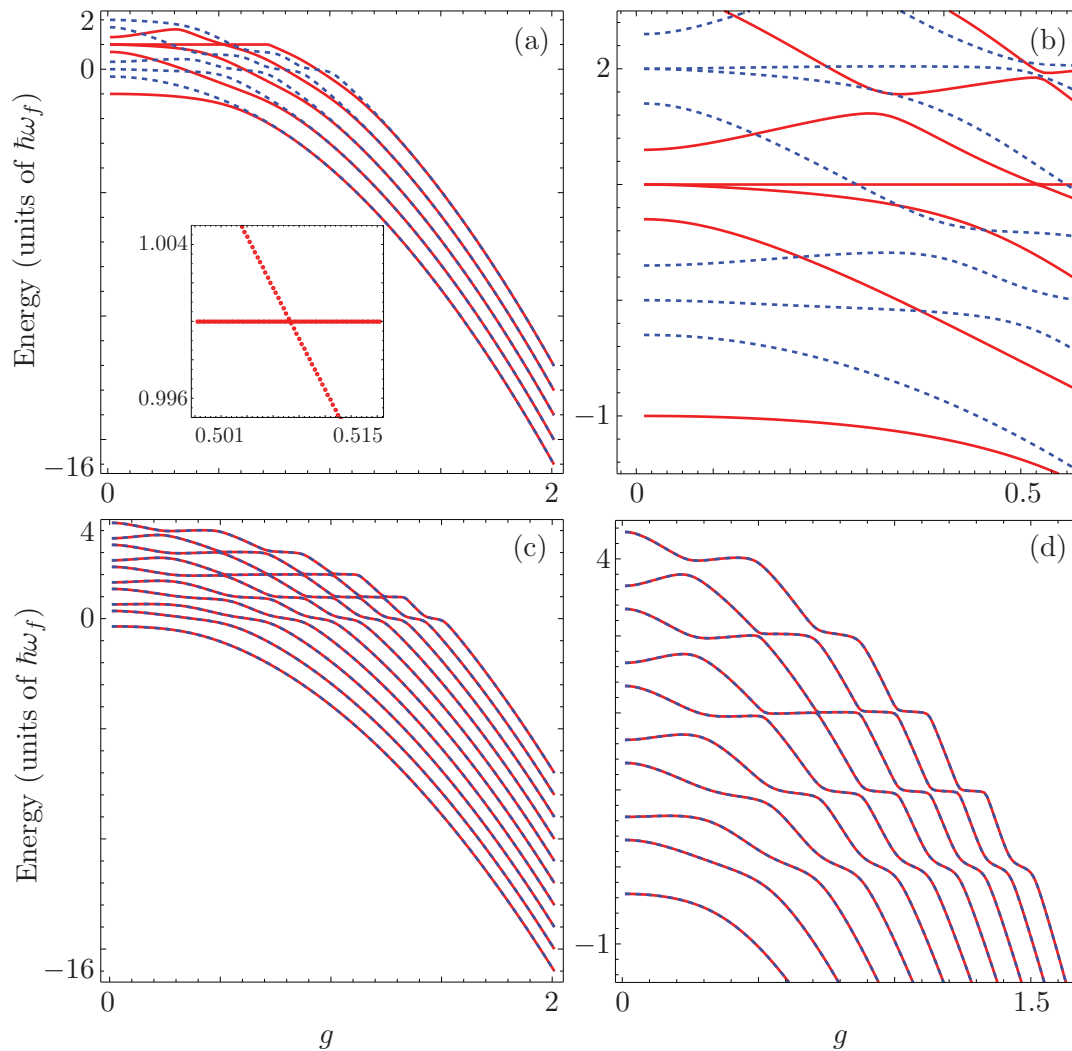


**Figure 2.** (Color online) Numerical spectra for the quantum Rabi Hamiltonian considering subspaces of up to one thousand excitations for even (solid red) and odd (dashed blue) parity subspaces for different parameter sets:  $\{\omega_1, \omega_2, g_1, g_2\} =$  (a) and (b)  $\{1.3, 0.7, g, g\}\omega_f$ , (c) and (d)  $\{0.7, 0, g, g\}\omega_f$ . The inset in (a) shows a crossing in the even parity spectra of the system. The driven oscillator behavior of the spectra, predicted by perturbation theory for extremely large values of the coupling parameters with respect to the transition frequencies, can already be seen for couplings twice as large as the transition frequencies for the lower eigenvalues.

parity subspaces were the norm and the spectra of the parity subspaces always cross each other. Also, in the cases of identical couplings,  $g_1 = g_2 = g$ , the lower eigenvalue branches already tend to the approximated spectra of two driven oscillator chains for not-so-large values of the coupling parameters; in the cases shown in Fig. 2(a) and 2(c) the first dozen eigenvalue branches already show this behavior for  $g_1 = g_2 \geq 2\omega_f$ .

### 3. Eigenstates of the model

Here we take on the calculation of the proper states of the system corresponding to the eigenvalues of the two-qubits quantum Rabi model. For the sake of completeness we use both a linear algebra and the Bargmann representation method that lead to four- and five-term recurrence relations between the coefficients of the eigenstates, respectively. The eigenstates provided by both methods are valid for any given coupling parameter value.

#### 3.1. Linear algebra approach

In order to calculate the proper functions of the model (3), let us use the fact that it conserves parity defined in (4). Then, it is trivial to extend the idea of a parity basis used in the single-qubit Rabi model [10, 11, 22],

$$|+, j\rangle = (\hat{V}^\dagger \hat{\sigma}_x)^j |0\rangle_f |g\rangle_1, \quad (19)$$

$$|-, j\rangle = (\hat{V}^\dagger \hat{\sigma}_x)^j |0\rangle_f |e\rangle_1, \quad (20)$$

where the Susskind-Glogower operator is defined as  $\hat{V}^\dagger = \sum_{k=0}^{\infty} |k+1\rangle \langle k|$  [39], such that we obtain an even and odd parity bases,

$$\{|j\rangle_+\} = \{|+, 0, g\rangle, |-, 0, e\rangle, |+, 1, g\rangle, |-, 1, e\rangle, |+, 2, g\rangle, |-, 2, e\rangle, \dots\}, \quad (21)$$

$$\{|j\rangle_-\} = \{|-, 0, g\rangle, |+, 0, e\rangle, |-, 1, g\rangle, |+, 1, e\rangle, |-, 2, g\rangle, |+, 2, e\rangle, \dots\}, \quad (22)$$

in that order, with  $\hat{\Pi}|j\rangle_\pm = \pm|j\rangle_\pm$ . The model Hamiltonian (3) in these bases,  $(H_\pm)_{j,k} = \langle j|\hat{H}|k\rangle_\pm$ , has block tridiagonal form:

$$H_\pm = \begin{pmatrix} D_0^\pm & O_1 & 0 & 0 & \dots \\ O_1 & D_1^\pm & O_2 & 0 & \dots \\ 0 & O_2 & D_2^\pm & O_3 & \dots \\ \vdots & \vdots & \vdots & \vdots & \vdots \end{pmatrix}, \quad (23)$$

where the blocks are given by

$$D_j^\pm = \begin{pmatrix} d_\pm^+ & 0 \\ 0 & d_\pm^- \end{pmatrix}, \quad O_j = \sqrt{j} \begin{pmatrix} g_1 & g_2 \\ g_2 & g_1 \end{pmatrix}. \quad (24)$$

with  $d_\pm^+ = j\omega_f \mp \frac{1}{2}[(-1)^j\omega_1 \pm \omega_2]$  and  $d_\pm^- = j\omega_f \pm \frac{1}{2}[(-1)^j\omega_1 \pm \omega_2]$ . Notice that the matrices  $O_j$  are invertible as long as  $|g_1|^2 \neq |g_2|^2$ . Thus, the eigenstates are written as

$$|\xi_+\rangle \propto \sum_{j=0}^{\infty} v_{j,0}^{(+)} |+, j, g\rangle + v_{j,1}^{(+)} |-, j, e\rangle, \quad (25)$$

$$|\xi_-\rangle \propto \sum_{j=0}^{\infty} v_{j,0}^{(-)} |-, j, g\rangle + v_{j,1}^{(-)} |+, j, e\rangle, \quad (26)$$

where we have used the symbol  $\xi_\pm$  to emphasize that the proper functions delivered by this method are valid for any given coupling parameter values. The coefficients can be

calculated up to a normalization factor by the four-term recurrence relations given by

$$\vec{v}_1^{(\pm)} = -O_1^{-1} (D_0^\pm - \mathbb{1}\xi_\pm) \vec{v}_0^{(\pm)}, \quad (27)$$

$$\vec{v}_j^{(\pm)} = -O_j^{-1} (D_{j-1}^\pm - \mathbb{1}\xi_\pm) \vec{v}_{j-1}^{(\pm)} - O_j^{-1} O_{j-1} \vec{v}_{j-2}^{(\pm)}, \quad j = 2, 3, \dots \quad (28)$$

by choosing a suitable  $\vec{v}_0^{(\pm)}$ , with  $\vec{v}_j^{(\pm)} = (v_{j,0}^{(\pm)}, v_{j,1}^{(\pm)})$  and using

$$O_j^{-1} (D_{j-1}^\pm - \mathbb{1}\xi_\pm) = \frac{1}{\sqrt{j}(g_1^2 - g_2^2)} \begin{pmatrix} g_1(d_\pm^+ - \xi_\pm) & -g_2(d_\pm^- - \xi_\pm) \\ -g_2(d_\pm^+ - \xi_\pm) & g_1(d_\pm^- - \xi_\pm) \end{pmatrix}, \quad (29)$$

$$O_j^{-1} O_{j-1} = \sqrt{\frac{j-1}{j}} \mathbb{1}, \quad (30)$$

where the symbol  $\mathbb{1}$  is the unitary matrix of dimension two.

Figure 3 shows the normalized ground state for the case of two nonidentical qubits off-resonance with the field frequency,  $\omega_1 = 1.1 \omega_f$  and  $\omega_2 = 0.3 \omega_f$ , for two strong-coupling parameters,  $g_1 = 3 \omega_f$  and  $g_2 = 4 \omega_f$ . For the sake of simplicity we have defined the normalized coefficients as  $u_{2j+k}^{(\pm)} \propto v_{j,k}^{(\pm)}$ . In this case the ground state energy is degenerate for even and odd parity chains,  $\xi_+ = \xi_- = -49.0052 \hbar\omega_f$ . Numerical evidence points to the fact that for large coupling parameters,  $g_1, g_2 \gg \omega_f$ , the ground state energy is degenerate for even and odd parity chains independent of the qubit transition frequency values,  $\omega_1$  and  $\omega_2$ . We want to emphasize that keeping track of the relative error is of great importance when calculating the eigenstates via the recurrence relations given in (27) and (28). A safer approach is to utilize standard linear algebra diagonalization packages for large sparse matrices.

### 3.2. Bargmann representation method

We can follow the procedure presented in [33] with our Hamiltonian model (3). That is, we use the transformation (8) to arrive to the rotated Hamiltonian,

$$\hat{H}_R = \hat{R}_y^\dagger \hat{H} \hat{R}_y, \quad (31)$$

$$= \omega_f \hat{a}^\dagger \hat{a} - \frac{1}{2} (\omega_1 \hat{\sigma}_x^{(1)} + \omega_2 \hat{\sigma}_x^{(2)}) + (\hat{a} + \hat{a}^\dagger) (g_1 \hat{\sigma}_z^{(1)} + g_2 \hat{\sigma}_z^{(2)}), \quad (32)$$

In the basis defined by  $\hat{\sigma}_z^{(1)}$  and using the Bargmann representation method, i.e., making the substitution  $\hat{a} \rightarrow \partial_z$  and  $\hat{a}^\dagger \rightarrow z$  where the shorthand notation  $\partial_x$  has been used to denote partial derivations with respect to  $x$ , this rotated Hamiltonian looks like

$$\hat{H}_R = \begin{pmatrix} \omega_f z \partial_z - \frac{\omega_2}{2} \sigma_x^{(2)} + (g_2 \sigma_z^{(2)} + g_1)(z + \partial_z) & -\frac{\omega_1}{2} \\ -\frac{\omega_1}{2} & \omega_f z \partial_z - \frac{\omega_2}{2} \sigma_x^{(2)} + (g_2 \sigma_z^{(2)} - g_1)(z + \partial_z) \end{pmatrix}. \quad (33)$$

Then, we can use the so-called Fulton-Gouterman transformation [40, 26, 33],

$$\hat{T}_{FG} = \frac{1}{\sqrt{2}} \begin{pmatrix} 1 & 1 \\ T_{FG} \sigma_x^{(2)} & -T_{FG} \sigma_x^{(2)} \end{pmatrix}, \quad (34)$$

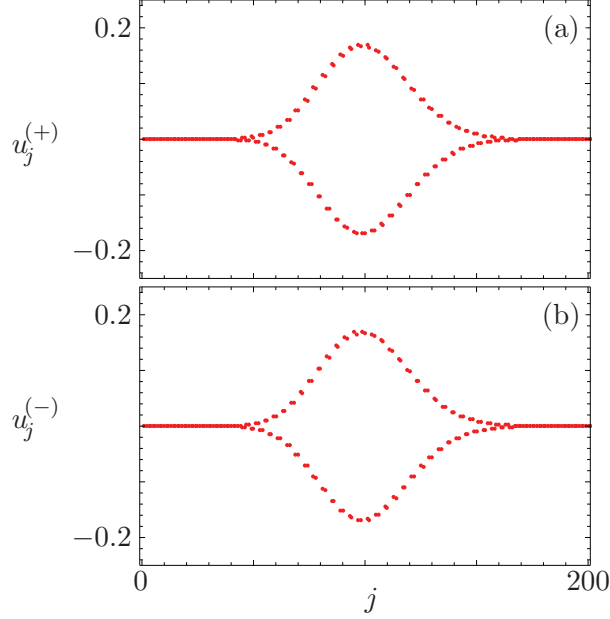


**Figure 3.** (Color online) The (a) even and (b) odd parity ground state coefficients for the quantum Rabi Hamiltonian considering a subspace of up to one thousand excitations for the parameter set  $\{\omega_1, \omega_2, g_1, g_2\} = \{1.1, 0.3, 3, 4\}\omega_f$ . The ground states are degenerate with energy  $\xi_{\pm} \approx -49.0052 \hbar\omega_f$ .

where the map  $T_{FG}$  is defined as  $T_{FG} : \phi(z) \rightarrow \phi(-z)$ . This procedure yields

$$\hat{T}_{FG}^\dagger \hat{H}_R \hat{T}_{FG} = \begin{pmatrix} H_- & 0 \\ 0 & H_+ \end{pmatrix} \quad (35)$$

with the auxiliary matrices given by

$$H_{\pm} = \begin{pmatrix} \omega_f z \partial_z + g_+(z + \partial_z) & -\frac{\omega_2}{2} \pm \frac{\omega_1}{2} T_{FG} \\ -\frac{\omega_2}{2} \pm \frac{\omega_1}{2} T_{FG} & \omega_f z \partial_z + g_-(z + \partial_z) \end{pmatrix}. \quad (36)$$

In other words, the eigenvalue problem is reduced to the form

$$H_{\pm} \begin{pmatrix} \phi_1^{\pm}(z) \\ \phi_2^{\pm}(z) \end{pmatrix} = \chi_{\pm} \begin{pmatrix} \phi_1^{\pm}(z) \\ \phi_2^{\pm}(z) \end{pmatrix}, \quad (37)$$

that can be written as the coupled differential equations,

$$[\omega_f z \partial_z + g_+(z + \partial_z) - \chi_{\pm}] \phi_1^{\pm} - \frac{\omega_2}{2} \phi_2^{\pm} \pm \frac{\omega_1}{2} \bar{\phi}_2^{\pm} = 0, \quad (38)$$

$$[\omega_f z \partial_z + g_-(z + \partial_z) - \chi_{\pm}] \phi_2^{\pm} - \frac{\omega_2}{2} \phi_1^{\pm} \pm \frac{\omega_1}{2} \bar{\phi}_1^{\pm} = 0, \quad (39)$$

and their sign inversion counterparts,

$$[\omega_f z \partial_z - g_+(z + \partial_z) - \chi_{\pm}] \bar{\phi}_1^{\pm} - \frac{\omega_2}{2} \bar{\phi}_2^{\pm} \pm \frac{\omega_1}{2} \phi_2^{\pm} = 0, \quad (40)$$

$$[\omega_f z \partial_z - g_-(z + \partial_z) - \chi_{\pm}] \bar{\phi}_2^{\pm} - \frac{\omega_2}{2} \bar{\phi}_1^{\pm} \pm \frac{\omega_1}{2} \phi_1^{\pm} = 0, \quad (41)$$

where we have used the shorthand notation  $\phi_j^{\pm} \equiv \phi_j^{\pm}(z)$  and  $\bar{\phi}_j^{\pm} = \phi_j^{\pm}(-z)$ . At this point we can take advantage of parity and use a pair of Bargmann functions with well defined

parity,  $\Phi_{j,\pm}^\pm = \phi_j^\pm \pm \bar{\phi}_j^\pm$  such that  $T_{FG}\Phi_{j,\pm}^\pm = \pm\Phi_{j,\pm}^\pm$ , that yield a coupled differential set,

$$[\omega_f z \partial_z - \chi_\pm] \Phi_{1,+}^\pm + g_+(z + \partial_z) \Phi_{1,-}^\pm - \frac{\omega_2 \mp \omega_1}{2} \Phi_{2,+}^\pm = 0, \quad (42)$$

$$[\omega_f z \partial_z - \chi_\pm] \Phi_{2,+}^\pm + g_-(z + \partial_z) \Phi_{2,-}^\pm - \frac{\omega_2 \mp \omega_1}{2} \Phi_{1,+}^\pm = 0, \quad (43)$$

$$[\omega_f z \partial_z - \chi_\pm] \Phi_{1,-}^\pm + g_+(z + \partial_z) \Phi_{1,+}^\pm - \frac{\omega_2 \pm \omega_1}{2} \Phi_{2,-}^\pm = 0, \quad (44)$$

$$[\omega_f z \partial_z - \chi_\pm] \Phi_{2,-}^\pm + g_-(z + \partial_z) \Phi_{2,+}^\pm - \frac{\omega_2 \pm \omega_1}{2} \Phi_{1,-}^\pm = 0, \quad (45)$$

that can be solved by Frobenius method with the power series solutions,

$$\Phi_{1,+}^\pm = \sum_{k=0}^{\infty} c_{2k}^\pm z^{2k}, \quad (46)$$

$$\Phi_{1,-}^\pm = \sum_{k=0}^{\infty} c_{2k+1}^\pm z^{2k+1}, \quad (47)$$

for one of the pairs of even and odd parity Bargmann functions; the coefficients for the other pair,  $\Phi_{2,\pm}^\pm$ , are obtained as functions of the coefficients  $c_k^\pm$  from (42) and (44). Such an approach yields a five-term recurrence relation for the coefficients  $c_k^\pm$ ,

$$\alpha_0^\pm(2)c_2^\pm + \alpha_1^\pm(2)c_1^\pm + \alpha_2^\pm(2)c_0^\pm = 0, \quad (48)$$

$$\alpha_0^\pm(3)c_3^\pm + \alpha_1^\pm(3)c_2^\pm + \alpha_2^\pm(3)c_1^\pm + \alpha_3^\pm(3)c_0^\pm = 0, \quad (49)$$

$$\alpha_0^\pm(j)c_j^\pm + \alpha_1^\pm(j)c_{j-1}^\pm + \alpha_2^\pm(j)c_{j-2}^\pm + \alpha_3^\pm(j)c_{j-3}^\pm + \alpha_4^\pm(j)c_{j-4}^\pm = 0, \quad j = 4, 5, \dots \quad (50)$$

with

$$\alpha_0^\pm(j) = \frac{j!}{(j-2)!} g_+ g_- [\omega_1 \mp (-1)^j \omega_2], \quad (51)$$

$$\alpha_1^\pm(j) = (j-1) \{ g_- [\omega_1 \mp (-1)^j \omega_2] [(j-1)\omega_f - \chi_\pm] + g_+ [\omega_1 \pm (-1)^j \omega_2] [\chi_\pm - (j-2)\omega_f] \}, \quad (52)$$

$$\alpha_2^\pm(j) = (2j-3)g_+g_- [\omega_1 \mp (-1)^j \omega_2] + [\omega_1 \pm (-1)^j \omega_2] \times \left\{ \frac{1}{4} [\omega_1 \mp (-1)^j \omega_2]^2 - [\chi_\pm - (j-2)\omega_f]^2 \right\}, \quad (53)$$

$$\alpha_3^\pm(j) = g_+ [\omega_1 \pm (-1)^j \omega_2] [\chi_\pm - (j-2)\omega_f] - g_- [\omega_1 \mp (-1)^j \omega_2] [\chi_\pm - (j-3)\omega_f], \quad (54)$$

$$\alpha_4^\pm(j) = g_+ g_- [\omega_1 \mp (-1)^j \omega_2]. \quad (55)$$

Notice that for the case of identical qubits,  $\omega_1 = \omega_2 = \omega_0$ , the differential set for the  $H_+$  block,

$$(\omega_f z \partial_z - \chi_+) \Phi_{1,+}^+ + g_+(z + \partial_z) \Phi_{1,-}^+ = 0, \quad (56)$$

$$(\omega_f z \partial_z - \chi_+) \Phi_{2,-}^+ - \omega_0 \Phi_{1,-}^+ = 0, \quad (57)$$

$$(\omega_f z \partial_z - \chi_+) \Phi_{1,-}^+ + g_+(z + \partial_z) \Phi_{1,+}^+ - \omega_0 \Phi_{2,-}^+ = 0, \quad (58)$$

$$(\omega_f z \partial_z - \chi_+) \Phi_{2,+}^+ = 0, \quad (59)$$

immediately shows us that the Bargman function  $\phi_2^+(z)$  has well defined odd parity as Eq.(59) accepts only the trivial solution  $\Phi_{2+}^+(z) = 0$ . In this case the five-term recurrence relations reduce to three-term recurrence relations for the coefficients, where we have rearranged the coefficients for the sake of simplicity,

$$c_j^\pm = \frac{1}{j} [\alpha_j^\pm c_{j-1}^\pm - (1 - \delta_{1,j}) c_{j-2}^\pm], \quad j = 1, 2, \dots \quad (60)$$

$$\alpha_j^\pm = \frac{[\chi_\pm - (j-1)\omega_f]^2 - \left[\frac{1 \pm (-1)^j}{2}\right]^2 \omega_0^2}{g_+ [\chi_\pm - (j-1)\omega_f]}. \quad (61)$$

Negative superindex corresponds to the differential set for the  $H_-$  block,

$$(\omega_f z \partial_z - \chi_-) \Phi_{1,-}^- + g_+(z + \partial_z) \Phi_{1,+}^- = 0, \quad (62)$$

$$(\omega_f z \partial_z - \chi_-) \Phi_{2,+}^- - \omega_0 \Phi_{1,+}^- = 0, \quad (63)$$

$$(\omega_f z \partial_z - \chi_-) \Phi_{1,+}^- + g_+(z + \partial_z) \Phi_{1,-}^- - \omega_0 \Phi_{2,+}^- = 0, \quad (64)$$

$$(\omega_f z \partial_z - \chi_-) \Phi_{2,-}^- = 0. \quad (65)$$

with  $\Phi_{1,+}^\pm = \sum_{j=0}^\infty c_{2j}^\pm z^{2j}$  and  $\Phi_{1,-}^\pm = \sum_{j=0}^\infty c_{2j+1}^\pm z^{2j+1}$ . Notice that the coefficients in the three-term recurrence relations satisfy  $\lim_{j \rightarrow \infty} \frac{\alpha_j^\pm}{\alpha_{j+1}^\pm} = 1$ .

## 4. Time Evolution

We want to include a way of calculating the exact time evolution in the RWA and show that numerical solutions for the full quantum problem are simplified by using the parity bases introduced in (21) and (22). In order to round up our example we show some typical measurements on radiation-matter interaction systems; e.g., mean photon number,  $\hat{n}$ , population inversion,  $\hat{S}_z = (\hat{\sigma}_z^{(1)} + \hat{\sigma}_z^{(2)})/2$ , von Neumann entropy of the bipartite system,  $\hat{S} = -\hat{\rho}_q \ln \hat{\rho}_q$ , and concurrence as defined by Wootters [41, 42].

### 4.1. Weak-coupling

Let us start from the Tavis-Cummings Hamiltonian for two-qubits in the frame defined by the transformation  $\hat{U}_{\hat{N}}(t) = e^{-i\omega_f \hat{N}t}$ ,

$$\hat{H}_{RWA} = \sum_{j=1,2} \Delta_j \hat{\sigma}_z^{(j)} + \sum_{j=1,2} g_j \left( \hat{a} \hat{\sigma}_+^{(j)} + \hat{a}^\dagger \hat{\sigma}_-^{(j)} \right), \quad (66)$$

where the detunings are given by  $\Delta_j = (\omega_j - \omega_f)/2$ . We have pointed out somewhere else [43] that the right unitary transformation,

$$\hat{T}_j = \begin{pmatrix} \hat{V} & 0 \\ 0 & 1 \end{pmatrix}_j, \quad (67)$$

diagonalizes the single-qubit Jaynes-Cummings model in the field basis. So, one can use that transformation for each qubit and obtain,

$$\left( \hat{T}_1 \otimes \hat{T}_2 \right) \hat{H}_{sc} \left( \hat{T}_2^\dagger \otimes \hat{T}_1^\dagger \right) = \hat{H}_{RWA}, \quad (68)$$

where

$$\hat{H}_{sc} = \begin{pmatrix} \Delta_1 + \Delta_2 & g_2\sqrt{n-1} & g_1\sqrt{n-1} & 0 \\ g_2\sqrt{n-1} & \Delta_1 - \Delta_2 & 0 & g_1\sqrt{n} \\ g_1\sqrt{n-1} & 0 & -\Delta_1 + \Delta_2 & g_2\sqrt{n} \\ 0 & g_1\sqrt{n} & g_2\sqrt{n} & -\Delta_1 - \Delta_2 \end{pmatrix}. \quad (69)$$

In order to obtain the evolution for this system, we can see that

$$\hat{H}_{RWA}^2 = \left( \hat{T}_1 \otimes \hat{T}_2 \right) \hat{H}_{sc} \left( \hat{T}_2^\dagger \otimes \hat{T}_1^\dagger \right) \left( \hat{T}_1 \otimes \hat{T}_2 \right) \hat{H}_{sc} \left( \hat{T}_2^\dagger \otimes \hat{T}_1^\dagger \right), \quad (70)$$

$$= \left( \hat{T}_1 \otimes \hat{T}_2 \right) \hat{H}_{sc}^2 \left( \hat{T}_2^\dagger \otimes \hat{T}_1^\dagger \right) - \left( \hat{T}_1 \otimes \hat{T}_2 \right) \hat{H}_{sc} \hat{R} \hat{H}_{sc} \left( \hat{T}_2^\dagger \otimes \hat{T}_1^\dagger \right), \quad (71)$$

$$= \left( \hat{T}_1 \otimes \hat{T}_2 \right) \hat{H}_{sc}^2 \left( \hat{T}_2^\dagger \otimes \hat{T}_1^\dagger \right) \quad (72)$$

with

$$\hat{R} = \begin{pmatrix} |0\rangle\langle 0| + |1\rangle\langle 1| & 0 & 0 & 0 \\ 0 & |0\rangle\langle 0| & 0 & 0 \\ 0 & 0 & |0\rangle\langle 0| & 0 \\ 0 & 0 & 0 & 0 \end{pmatrix}, \quad (73)$$

which leads us to write the evolution operator of the system in the RWA as

$$\hat{U}_{RWA}(t) = \left( \hat{T}_1 \otimes \hat{T}_2 \right) e^{-i\hat{H}_{sc}t} \left( \hat{T}_2^\dagger \otimes \hat{T}_1^\dagger \right). \quad (74)$$

This requires just to keep track of the action of  $\left( \hat{T}_2^\dagger \otimes \hat{T}_1^\dagger \right)$  over the given initial state in order to calculate its evolution. It is simple to calculate the exponential because the Hamiltonian  $\hat{H}_{sc}$  has a depressed quartic as characteristic polynomial,

$$|H_{sc} - \lambda I| = c_0 + c_1\lambda + c_2\lambda^2 + \lambda^4, \quad (75)$$

$$c_0 = [n(g_1^2 - g_2^2) + \Delta_1^2 - \Delta_2^2] [(n-1)(g_1^2 - g_2^2) + \Delta_1^2 - \Delta_2^2], \quad (76)$$

$$c_1 = 2(g_2^2\Delta_1 + g_1^2\Delta_2), \quad (77)$$

$$c_2 = (1 - 2n)(g_1^2 + g_2^2) - 2(\Delta_1^2 + \Delta_2^2), \quad (78)$$

with roots,

$$\lambda_{1,2} = \frac{p \pm \sqrt{-p^2 - 2c_2 - 2c_1/p}}{2}, \quad (79)$$

$$\lambda_{3,4} = \frac{-p \pm \sqrt{-p^2 - 2c_2 + 2c_1/p}}{2}, \quad (80)$$

and parameters,

$$p = \sqrt{\frac{12c_0 + (c_2 - c)^2}{3c}}, \quad (81)$$

$$c = \left[ \frac{1}{2}(q + 27c_1^2 - 72c_0c_2 + 2c_2^3) \right]^{1/3}, \quad (82)$$

$$q = \sqrt{(27c_1^2 - 72c_0c_2 + 2c_2^3)^2 - 4(12c_0 + c_2^2)^3}. \quad (83)$$

Once the eigenvalues are obtained, it is trivial but cumbersome to calculate the eigenstates of  $\hat{H}_{sc}$  that allow us to write the evolution operator  $\hat{U}(t)$ . For the sake

of giving an example, let us take the peculiar and simple case when the initial state is a Fock state with the two-qubits in the ground state,  $|\psi(0)\rangle = |n, g, g\rangle$ , with symmetric detunings,  $\Delta_1 = -\Delta_2 = \Delta$ , and identical couplings,  $g_1 = g_2 = g$ , two of the eigenvalues are zero and the other two are  $\lambda_{\pm} = \pm 2\sqrt{\Delta^2 + g^2(n - 1/2)}$ . So, we can write the time evolution of the state as

$$|\psi(t)\rangle = \left( \begin{array}{c} \frac{g^2\sqrt{(\hat{n}+2)(\hat{n}+1)}}{\Omega^2(\hat{n}+2)} (\cos \Omega(\hat{n} + 2)t - 1) \hat{V}^2 \\ \frac{g\sqrt{\hat{n}+1}}{\Omega^2(\hat{n}+1)} [\Delta (\cos \Omega(\hat{n} + 1)t - 1) - \frac{i}{2}\Omega(\hat{n} + 1) \sin \Omega(\hat{n} + 1)t] \hat{V} \\ \frac{g\sqrt{\hat{n}+1}}{\Omega^2(\hat{n}+1)} [-\Delta (\cos \Omega(\hat{n} + 1)t - 1) - \frac{i}{2}\Omega(\hat{n} + 1) \sin \Omega(\hat{n} + 1)t] \hat{V} \\ \frac{1}{\Omega^2(\hat{n})} [2\Delta^2 + g^2(\hat{n} - 1) + g^2\hat{n} \cos \Omega(\hat{n})t] \end{array} \right) |n\rangle, \quad (84)$$

with the Rabi frequency defined as  $\Omega(\hat{n}) = |\lambda_{\pm}| = 2\sqrt{\Delta^2 + g^2(\hat{n} - 1/2)}$ . Notice that these initial conditions give  $\langle \hat{\sigma}_{z(y)}^{(1)} \rangle = \langle \hat{\sigma}_{z(y)}^{(2)} \rangle$  and  $\langle \hat{\sigma}_x^{(1)} \rangle = -\langle \hat{\sigma}_x^{(2)} \rangle$ .

For more general parameter sets in the weak-coupling regime, let us consider an initial state example given by a coherent field plus the qubits in the ground state,  $|\psi(0)\rangle = |\alpha, g, g\rangle$ , the transformation applied over this state acts like the identity,  $(\hat{T}_2^\dagger \otimes \hat{T}_1^\dagger) |\psi(0)\rangle = |\psi(0)\rangle$ . In Fig. 4 we show the time evolution for the mean photon number, population inversion, von Neuman entropy and qubit bipartite concurrence for the case of two nonidentical qubits,  $\omega_1 = 1.1\omega_f$  and  $\omega_2 = 0.3\omega_f$ , weakly coupled to the field,  $g_1 = 0.03\omega_f$  and  $g_2 = 0.04\omega_f$ . One can see that the collapse and revival of the population inversion, characteristic of such an initial state, is not as strong as in the case of equal qubits [43]. The fast modulation of the curves is an interesting feature that does not occur in the identical qubits case [43]. The von Neuman entropy points to entanglement between the qubit ensemble and the quantum field. The qubits bipartite concurrence tells us that quantum correlations between the qubits are created by interaction with the field but the qubit ensemble is close to being separable.

#### 4.2. Parity based numeric approach

In the most general case of any given coupling parameter set, one can approximate results by adequately truncating the  $\hat{H}_{\pm}$  matrices in (23) obtained by using the parity bases (21) and (22). This numerical approach allows us to calculate the time evolution of a general initial state decomposed in the even and odd parity chain bases, respectively,

$$|\psi(0)\rangle_+ = \sum_{n=0}^{\infty} c_n^{(+)} |n\rangle_+, \quad (85)$$

$$\begin{aligned} &= \sum_{n=0}^{\infty} c_{4n}^{(+)} |2n, g, g\rangle + c_{4n+1}^{(+)} |2n, e, e\rangle + \\ &\quad + c_{4n+2}^{(+)} |2n+1, e, g\rangle + c_{4n+3}^{(+)} |2n+1, g, e\rangle, \end{aligned} \quad (86)$$

$$|\psi(0)\rangle_- = \sum_{n=0}^{\infty} c_n^{(-)} |n\rangle_-, \quad (87)$$

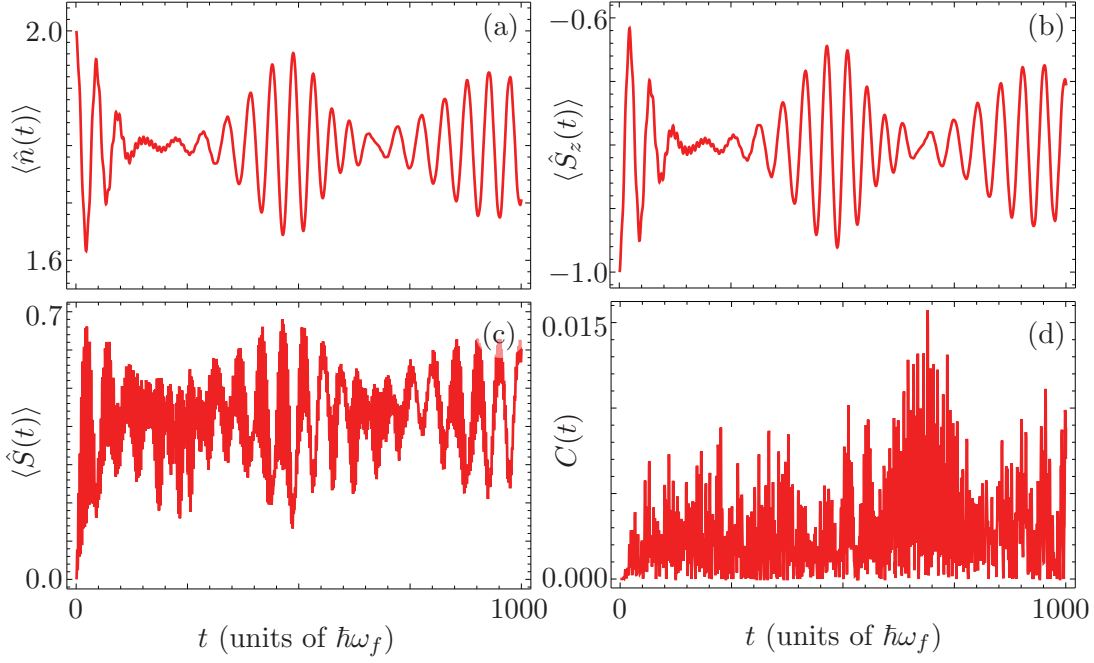


**Figure 4.** (Color online) The time evolution of the (a) mean photon number, (b) population inversion, (c) von Neuman entropy and (d) bipartite concurrence for a quantum Rabi Hamiltonian under the RWA with the parameter set  $\{\omega_1, \omega_2, g_1, g_2\} = \{1.1, 0.3, 0.03, 0.04\}\omega_f$  and initial state  $|\phi(0)\rangle = |\alpha, g, g\rangle$  with  $\alpha = \sqrt{2}$ .

$$\begin{aligned}
 &= \sum_{n=0}^{\infty} c_{4n}^{(-)} |2n, e, g\rangle + c_{4n+1}^{(-)} |2n, g, e\rangle + \\
 &\quad + c_{4n+2}^{(-)} |2n+1, g, g\rangle + c_{4n+3}^{(-)} |2n+1, e, e\rangle
 \end{aligned} \tag{88}$$

with the prescription,

$$\vec{c}^{(\pm)}(t) = e^{-i\hat{H}_{\pm}t} \vec{c}^{(\pm)}(0), \tag{89}$$

where the notation  $\vec{c}^{(\pm)}$  corresponds to a vector of state amplitudes. The average photon number of the field is then given by

$$\langle \hat{n}(t) \rangle = \langle \hat{n}(t) \rangle_+ + \langle \hat{n}(t) \rangle_-, \tag{90}$$

$$\langle \hat{n}(t) \rangle_{\pm} = \sum_{n=0}^{\infty} 2n \left( |c_{4n}^{(\pm)}|^2 + |c_{4n+1}^{(\pm)}|^2 \right) + (2n+1) \left( |c_{4n+2}^{(\pm)}|^2 + |c_{4n+3}^{(\pm)}|^2 \right), \tag{91}$$

any other quantity of interest can be calculated from the qubit ensemble reduced density matrix,  $\hat{\rho}_q = \sum_n {}_f \langle n | \hat{\rho} | n \rangle_f = \hat{\rho}_q^{(+)} + \hat{\rho}_q^{(-)}$  with  $\hat{\rho} = \hat{\rho}^{(+)} + \hat{\rho}^{(-)}$ , in the  $\hat{\sigma}_z^{(1)} \otimes \hat{\sigma}_z^{(2)}$  basis,

$$\hat{\rho}_q^{(+)} = \sum_{n=0}^{\infty} \begin{pmatrix} |c_{4n+1}^{(+)}|^2 & c_{4n+1}^{(+)*} c_{4n+2}^{(+)} & c_{4n+1}^{(+)} c_{4n+3}^{(+)*} & c_{4n+1}^{(+)} c_{4n}^{(+)*} \\ c_{4n+2}^{(+)} c_{4n+1}^{(+)*} & |c_{4n+2}^{(+)}|^2 & c_{4n+2}^{(+)} c_{4n+3}^{(+)*} & c_{4n+2}^{(+)} c_{4n}^{(+)*} \\ c_{4n+3}^{(+)} c_{4n+1}^{(+)*} & c_{4n+3}^{(+)} c_{4n+2}^{(+)*} & |c_{4n+3}^{(+)}|^2 & c_{4n+3}^{(+)} c_{4n}^{(+)*} \\ c_{4n}^{(+)} c_{4n+1}^{(+)*} & c_{4n}^{(+)} c_{4n+2}^{(+)*} & c_{4n}^{(+)} c_{4n+3}^{(+)*} & |c_{4n}^{(+)}|^2 \end{pmatrix}, \tag{92}$$

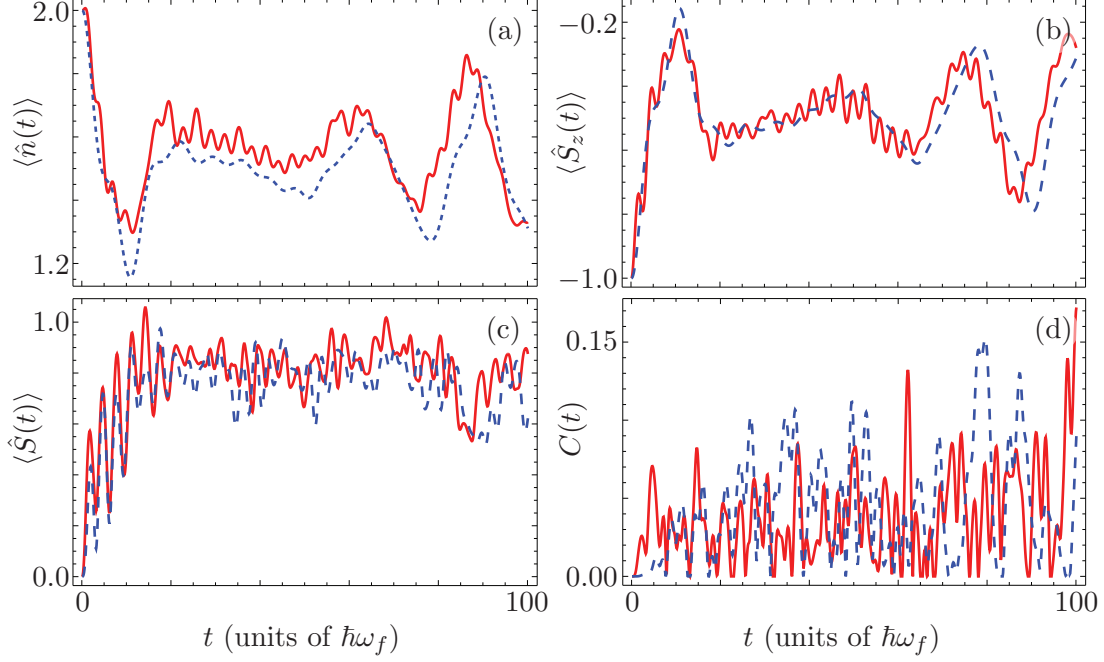


**Figure 5.** (Color online) The time evolution of the (a) mean photon number, (b) population inversion, (c) von Neuman entropy and (d) bipartite concurrence for a RWA Hamiltonian (dashed blue) and a quantum Rabi Hamiltonian (solid red) with the parameter set  $\{\omega_1, \omega_2, g_1, g_2\} = \{1.1, 0.3, 0.1, 0.15\}\omega_f$  and initial state  $|\phi(0)\rangle = |\alpha, g, g\rangle$  with  $\alpha = \sqrt{2}$ .

$$\hat{\rho}_q^{(-)} = \sum_{n=0}^{\infty} \begin{pmatrix} |c_{4n+3}^{(-)}|^2 & c_{4n+3}^{(-)} c_{4n}^{(-)*} & c_{4n+3}^{(-)} c_{4n+1}^{(-)*} & c_{4n+3}^{(-)} c_{4n+2}^{(-)*} \\ c_{4n}^{(-)} c_{4n+3}^{(-)*} & |c_{4n}^{(-)}|^2 & c_{4n}^{(-)} c_{4n+1}^{(-)*} & c_{4n}^{(-)} c_{4n+2}^{(-)*} \\ c_{4n+1}^{(-)*} c_{4n+3}^{(-)} & c_{4n+1}^{(-)*} c_{4n}^{(-)} & |c_{4n+1}^{(-)}|^2 & c_{4n+1}^{(-)*} c_{4n+2}^{(-)*} \\ c_{4n+2}^{(-)} c_{4n+3}^{(-)*} & c_{4n+2}^{(-)} c_{4n}^{(-)*} & c_{4n+2}^{(-)} c_{4n+1}^{(-)*} & |c_{4n+2}^{(-)}|^2 \end{pmatrix}. \quad (93)$$

In Fig. 5 we show a comparison between the dynamics given by the RWA and the full quantum Rabi Hamiltonian for coupling parameters near to 10% of the field frequency value. One can see that the RWA fails in providing a detailed description of the dynamics as mentioned above and in [36]. Figure 6 presents the dynamics given by the quantum Rabi Hamiltonian for strong-coupling parameters, one can see a great deviation in the behavior from the weak-coupling dynamics presented in Fig. 4 where the couplings are a hundred times smaller. Note that the quantum correlations between the qubit and the field and between the qubits increase with respect to the weak-coupling case.

## 5. Conclusion

This manuscript was motivated by the results of [33], where the assumption  $\omega_2 = 0$  is made in order to deliver three-term recurrence relations and Green functions similar in form to those presented by [26] for the single-qubit case. We wanted to show that it is possible to study a proper, physical two-qubit quantum Rabi Hamiltonian by extending

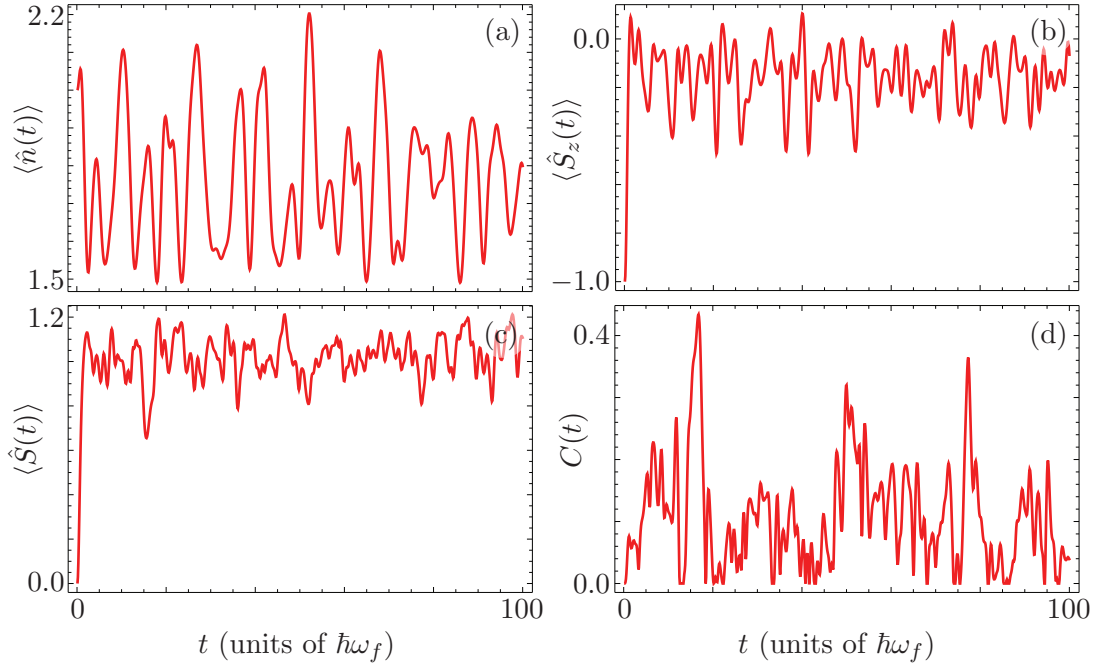


**Figure 6.** (Color online) The time evolution of the (a) mean photon number, (b) population inversion, (c) von Neuman entropy and (d) bipartite concurrence for a quantum Rabi Hamiltonian with the parameter set  $\{\omega_1, \omega_2, g_1, g_2\} = \{1.1, 0.3, 3, 4\}\omega_f$  and initial state  $|\phi(0)\rangle = |\alpha, g, g\rangle$  with  $\alpha = \sqrt{2}$  considering a subspace of up to one thousand excitations.

well known methods for single-qubit models that exist in the literature since [8, 9].

We have shown the well-known result that the spectra of the two-qubit quantum Rabi model in the weak-coupling regime is easily obtained by partitioning the Hilbert space in manifolds of constant total number of excitation, a standard procedure in the single-qubit quantum Rabi problem [10]. Our main results are the following. In the strong-coupling regime we have calculated the eigenvalues up to second order perturbation correction. An interesting result occurs for ultrastrong-couplings where the eigenvalues of the two-qubit Rabi model are described by two forced oscillator spectral series; this is equivalent to what happens in the single-qubit case [8, 11]. In the intermediate regime, partitioning the Hilbert space in even and odd parity subspaces simplifies the numerical calculation of the eigenvalues; an interesting result from numeric evidence is that the ground state of even and odd subspaces is degenerate for coupling values larger than the field frequency value. The numerical spectra points to energy crossings within and between each of the parity subspaces with moderate couplings. This is a different behavior to that of the single-qubit results, where the spectra branches within each of the parity subspaces do not cross and the parity subspaces spectra cross each other [11, 26]. We have obtained the normal modes for the two-qubit Rabi model by linear algebra methods via parity subspaces as four-terms recurrence relations for the coefficients of the eigenstates; in the case of identical couplings the linear system becomes singular and we cannot provide an analytic solution, nevertheless it is possible to obtain

numeric solutions for this particular case. In Bargmann representation, we find that the recurrence relation for the continued proper functions coefficients are five-term and reduce to three-term recurrence relations in the case of identical qubits; additionally, for identical qubits, one of the proper functions has well defined parity. Finally, we wanted to show how powerful the parity decomposition is by calculating the time evolution of quantities related to the degree of entanglement in the ensemble-field and qubit system for a simple initial state of the qubits in their ground state and the field in a coherent state with two photons on average under weak-, moderate- and strong-coupling.

## Acknowledgments

BMRL is grateful to Rocío Jáuregui and Carlos Pineda for useful discussion and comments.

## References

- [1] Dicke R H 1954 *Phys. Rev.* **93** 99 – 110
- [2] Tavis M and Cummings F W 1968 *Phys. Rev.* **170** 170 – 176
- [3] Garraway B M 2011 *Phil. Trans. R. Soc. A* **369** 1137 – 1155
- [4] Dimer F, Estienne B, Parkins A S and Carmichael H J 2007 *Phys. Rev. A* **75** 013804
- [5] Nagy D, Szirmai G and Domokos P 2008 *Eur. Phys. J. D* **48** 127 – 137
- [6] Baumann K, Guerlin C, Brennecke F and Esslinger T 2010 *Nature* **464** 1301 – 1306
- [7] Nagy D, Konya G, Szirmai G and Domokos P 2010 *Phys. Rev. Lett.* **104** 130401
- [8] Schweber S 1967 *Ann. Phys.* **41** 205 – 229
- [9] Swain S 1973 *J. Phys. A: Math. Nucl. Gen.* **6** 1919 – 1934
- [10] Tur E A 2000 *Opt. Spectrosc.* **89** 574 – 588
- [11] Tur E A 2001 *Opt. Spectrosc.* **91** 899 – 902
- [12] Graham R and Höhnerbach M 1984 *Z. Phys. B Cond. Mat.* **57** 233 – 248
- [13] Zaheer K and Zubairy M S 1988 *Phys. Rev. A* **37** 1628 – 1633
- [14] Phoenix S J D 1989 *J. Mod. Opt.* **36** 1163–1172
- [15] Bishop R F, Davidson N J, Quick R M and van der Walt D M 1996 *Phys. Rev. A* **54** R4657 – R4660
- [16] Zeng L, Liu Z, Lin Y and Zhu S 1998 *Phys. Lett. A* **246** 43 – 51
- [17] Zheng H, Zhu S Y and Zubairy M S 2008 *Phys. Rev. Lett.* **101** 200404
- [18] Wang D W, Li A J, Wang L G, Zhu S Y and Zubairy M S 2009 *Phys. Rev. A* **80** 063826
- [19] Englund D, Faraon A, Fushman I, Stoltz N, Petroff P and Vučković J 2007 *Nature* **450** 857 – 861
- [20] Bourassa J, Gambetta J M, Jr A A A, Astafiev O, Nakamura Y and Blais A 2009 *Phys. Rev. A* **80** 032109
- [21] Niemczyk T, Deppe F, Huebl H, Menzel E P, Hocke F, Schwarz M J, Garcia-Ripoll J J, Zueco D, Hümmer T, Solano E, Marx A and Gross R 2010 *Nature Phys.* **6** 772 – 776
- [22] Casanova J, Romero G, Lizuain I, García-Ripoll J J and Solano E 2010 *Phys. Rev. Lett.* **105** 263603
- [23] Yu L, Zhu S, Liang Q, Chen G and Jia S 2012 *Phys. Rev. A* **86** 015803
- [24] Pan F, Guan X, Wang Y and Draayer J P 2010 *J. Phys. B: At. Mol. Opt. Phys.* **43** 175501
- [25] Ziegler K 2012 *J. Phys. A: Math. Theor.* **45** 452001
- [26] Braak D 2011 *Phys. Rev. Lett.* **107** 100401
- [27] Moroz A 2012 Comment on "Integrability of the Rabi model" arXiv: 1205.3139

- [28] Maciejewski A J, Przybylska M and Stachowiak T 2012 How to calculate spectra of rabi and related models arXiv: 1210.1130
- [29] Braak D 2012 Note on the analytical solution of the Rabi model arXiv:1210.4946 [math-ph]
- [30] Maciejewski A J, Przybylska M and Stachowiak T 2012 Comment on “Note on the analytical solution of the rabi model” arXiv: 1211.4639 [quant-ph]
- [31] Wolf F A, Kollar M and Braak D 2012 *Phys. Rev. A.* **85** 053817
- [32] Chen Q H, Wang C, He S, Liu T and Wang K L 2012 *Phys. Rev. A* **86** 023822
- [33] Peng J, Ren Z, Guo G and Ju G 2012 *J. Phys. A: Math. Theor.* **45** 365302
- [34] Sillanpää M A, Park J I and Simmonds R W 2007 *Nature* **449** 438 – 442
- [35] Haack G, Helmer F, Mariani M, Marquardt F and Solano E 2010 *Phys. Rev. B* **82** 024514
- [36] Wang Y M, Ballester D, Romero G, Scarani V and Solano E 2012 *Phys. Sc* **T147** 014031
- [37] Altintas F and Eryigit R 2012 *Phys. Lett. A* **376** 1791 – 1796
- [38] Bargmann V 1947 *Ann. Math.* **48** 568 – 640
- [39] Susskind L and Glogower J 1964 *Physics* **1** 49 – 61
- [40] Fulton R L and Gouterman M 1961 *J. Chem. Phys.* **35** 1059 – 1071
- [41] Wootters W K 1998 *Phys. Rev. Lett.* **80** 2245 – 2248
- [42] Wootters W K 2001 *Quantum Inf. Comput.* **1** 27–44
- [43] Rodríguez-Lara B M and Moya-Cessa H M 2012 Exact solution of generalized dicke models via susskind-glogower operators arXiv:1207.6551 (Accepted J. Phys. A: Math. Theor. January 18th 2013)